IOP Conf. Series: Materials Science and Engineering **117** (2016) 012037 doi:10.1088/1757-899X/117/1/012037

Numerical simulation of casting process to assist in defects reduction in complex steel tidal power component

E J Guo, S C Zhao[a], L P Wang, T Wu, B P Xin, J J Tan and H L Jia
School of Materials Science and Engineering, Harbin University of Science and Technology, No.4 Linyuan Road, Xiangfang District, Harbin150040, Heilongjiang Province, People's Republic of China

E-mail: [a] zscwr@163.com

Abstract. In order to reduce defects and improve casting quality, ProCAST software is performed to study the solidification process of discharge bowl. Simulated results of original casting process show that the hot tearing is serious at the intersection of blades and outer or inner rings. The shrinkage porosity appears at the bottom of discharge bowl and the transition area of wall thickness. Based on the formation mechanisms of the defects, the structure of chills attached on the outer surface of discharge bowl casting is optimized. The thickness of chills ranges from 25mm to 35mm. The positions of chills corresponded to the outer surface of the T-shaped parts. Compared to the original casting design (without chills), the hot tearing and shrinkage porosity of the discharge bowl are greatly improved with addition of chills.

1. Introduction

The tidal power devices are demanded higher performance with the rapid development of tidal power technologies. The discharge bowl is a key component of tidal power devices. The material of the discharge bowl is CD4MCu duplex stainless steel [1]. Although this material is resistant to corrosion and good mechanical properties, casting performance is poor. However, only the sand casting method is suitable for producing the discharge bowl, because the structure of the discharge bowl is complex. The diameter of the discharge bowl is 1700mm. The thickness of the blades are about 20mm. The hot tearing is serious at the intersection of blades and outer or inner rings. The shrinkage porosity appears at the bottom of the discharge bowl and the transition area of wall thickness. These defects seriously degrade the mechanical properties and quality of castings. Therefore, it is necessary to research the formation mechanisms of hot tearing and shrinkage porosity and find ways to reduce these defects of discharge bowl casting. Although physical experiment is a possible way, it is still difficult to use those experiments to explain the results in the real castings because of the opaqueness of the alloy melt [2, 3]. Therefore, the ProCAST software is used to study the solidification of discharge bowl casting.

2. Model and boundary conditions

The 3D model of discharge bowl casting should be meshed, and the boundary and initial conditions should be determined before calculation. The 3D model of casting is meshed by Hypermesh. The total number of grid is about 2 million. The material of discharge bowl is CD4MCu, which thermophysical properties come from the Magmasoft's built-in database. The temperature of chills and ambient is 25℃. Thermal, flow and stress modules are activated in run parameters.

IOP Conf. Series: Materials Science and Engineering **117** (2016) 012037 doi:10.1088/1757-899X/117/1/012037

3. Numerical simulation of the original casting process

The solidification process and temperature field of the original casting process are shown in figure 1. Red indicates the highest temperature of 1580 ℃. Purple indicates the solidus temperature of 1370℃. Due to the thickness of blades, outer ring, inner ring and bottom ring is smallest, the cooling rate of them are fastest. However, because the center of the feeder is the location of hot spot, the cooling rate and time of feeders are slowly and long.

The locations of three key points are shown in figure 2. The point 1, point 2 and point 3 locate in the intersection of the blade and the bottom ring, the blade and the inner ring and the blade and the outer ring, respectively.

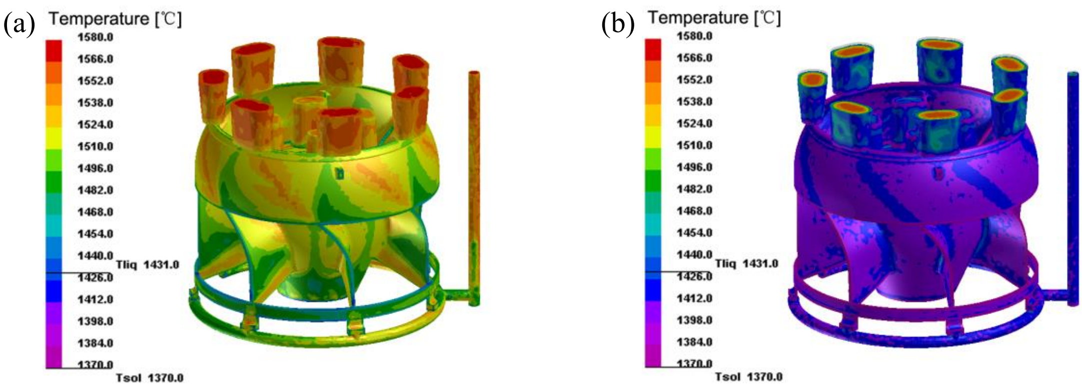

Figure 1. The solidification process and temperature field of the original casting process. (a) 7s after filling, (b) 90s after filling.

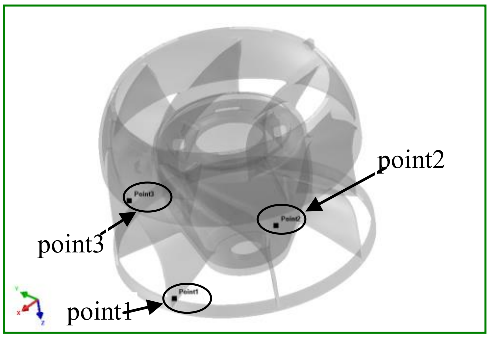

Figure 2. The locations of three key points.

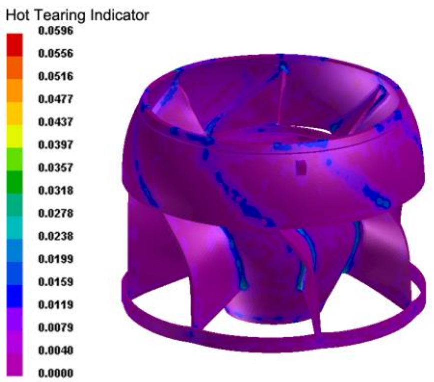

Figure 3. Hot tearing indicator of original casting process.

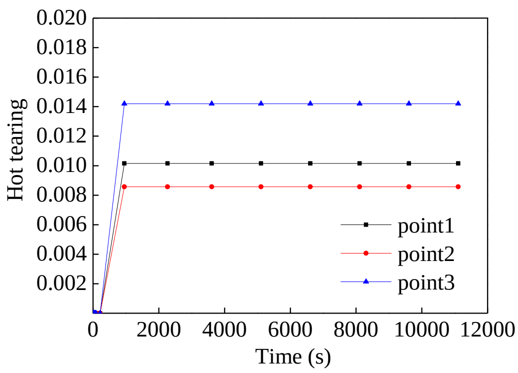

Figure 4. Hot tearing indicator curves of original casting process.

The hot tearing indicator of the original casting process is shown in figure 3. The hot tearing indicator is based on the physics of solidification and deformation. Hot tearing forms when the mushy zone is starved of liquid feeding and deformed in tension. The unfed tensile deformation causes a small additional porosity. This additional porosity or porosity due to solid deformation is a locator for initiation sites for hot tears in the casting [4]. Simulated results show that the hot tearing is serious at the intersection of blades and outer or inner rings (T-shaped parts). The T-shaped parts are the transition zones of wall thickness. The cooling rate of T-shaped parts is uniformity, so the large stress is formed. Hot tearing indicator curves of original casting process are shown in figure 4. The value of hot tearing tendency of point3 is higher than point 2 or point 1. Effective stress and effective plastic strain of original casting process are shown in figure 5. If the value of effective stress is higher than the strength of the alloy, the hot tearing would be generated in T-shaped parts.

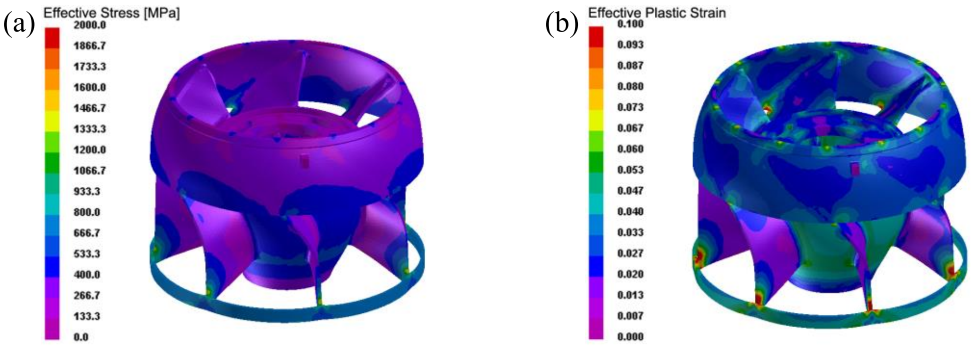

Figure 5. Effective stress and effective plastic strain of original casting process. (a) Effective stress, (b) Effective plastic strain.

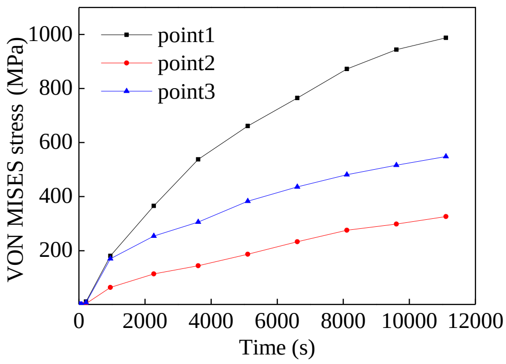

Figure 6. The Von Mises stress curves of original casting process.

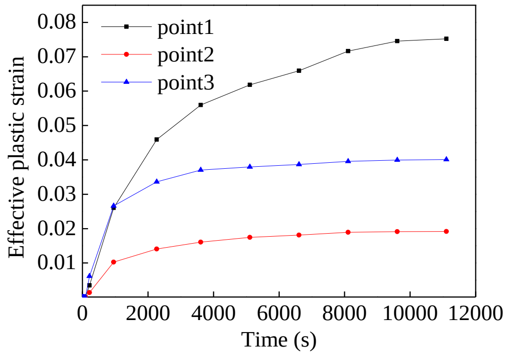

Figure 7. Effective plastic strain curves of original casting process.

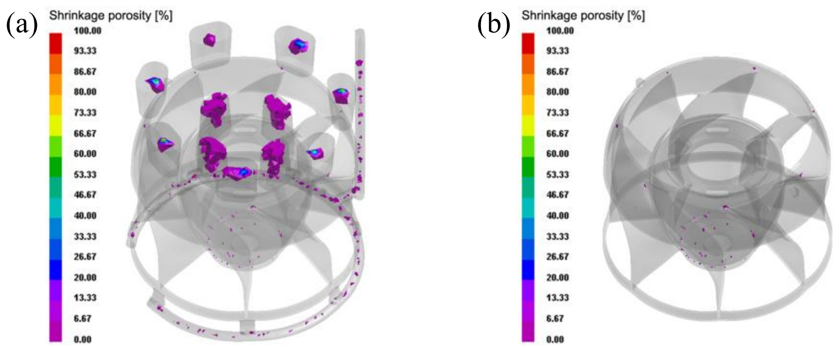

Figure 8. Shrinkage porosity predicted of original casting process. (a) Overall view, (b) Partial view.

The Von Mises stress and effective plastic strain curves of original casting process are shown in figure 6 and figure 7, respectively. The Von Mises stress and effective plastic strain increase over time. Shrinkage porosity predicted of original casting process is shown in figure 8. Shrinkage porosity is quantitatively predictable by Magmasoft's built-in "shrinkage porosity criterion" function. The criterion function automatically calculates the degree of solidification shrinkage and feeding for each of the control volumes [5]. The shrinkage porosity appears at feeders, runners, bottom of discharge bowl and the T-shaped parts.

4. The optimized parameters of chills and simulation results

4.1. The basic principle of reducing hot tearing by chills

Schematic diagram of reducing hot tearing is shown in figure 9. The temperature of T-shaped parts is higher than the adjacent regions. This indicates that the solidification time of T-shaped parts is longer than blades. The T-shaped parts are easy to generate hot tearing, the reasons may be the solidified regions (blades) generate larger linear shrinkage than mushy regions (T-shaped parts) in solidification process, and the tensile strength of mushy regions is smaller than solidified regions. If the chills are well attached on the outer surface of transition regions, the solidification sequence of T-shaped parts would be as same as blades. Therefore, the hot tearing will be effectively reduced by chills.

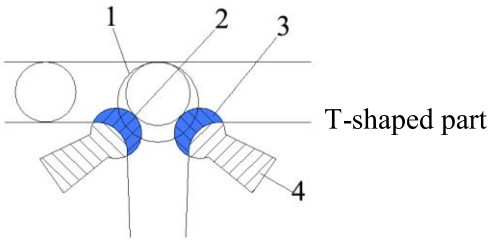

Figure 9. Schematic diagram of reducing hot tearing. 1- Inscribed circle is not chilled, 2- Inscribed circle is chilled, 3- The chilled regions, 4- Chills.

4.2. The optimized parameters of chills

Based on the formation mechanisms the defects, the structure and position of chills attached on the outer surface of discharge bowl casting are optimized. The thickness of chills ranges from 25mm to 35mm. The positions of chills correspond to the outer surface of the T-shaped parts. The material of chills is steel. The optimized structure of chills is shown in figure 10.

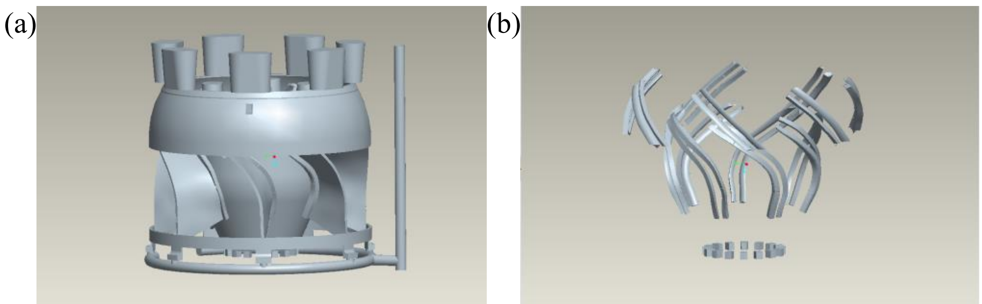

Figure 10. The optimized structure of chills. (a) Foundry methods drawing, (b) Structure drawing of chills.

4.3. Simulation results after optimization

Pouring temperature is 1580℃, and filling time is 30s. The solidification process and temperature field after optimization is shown in figure 11. T-shaped parts are chilled in the solidification process. The hot tearing indicator after optimization is shown in figure 12. The hot tearing of T-shape parts is significantly reduced. The hot tearing indicator curves after optimization is shown in figure 13. Compared with the simulation results without chills, the hot tearing value of point 1, point 2 and point 3 decrease from 0.010 to 0.004, 0.008 to 0.0005 and 0.014 to 0.005, respectively. The change in hot tearing value of point2 is largest. The value of hot tearing of three key points is reduced by at least an order of magnitude.

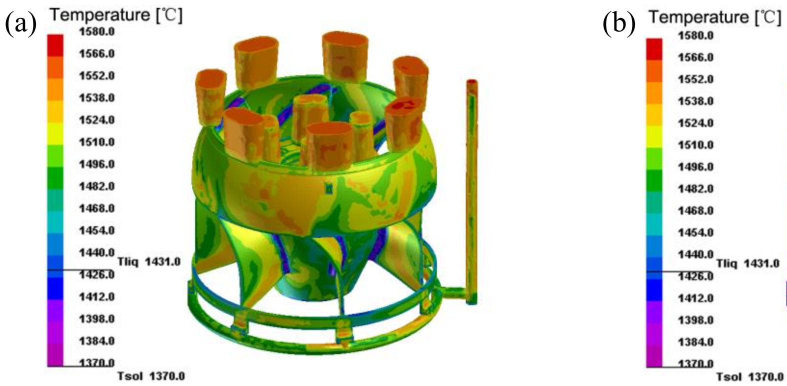

Figure 11. The solidification process and temperature field after optimization. (a) 7s after filling, (b) 90s after filling.

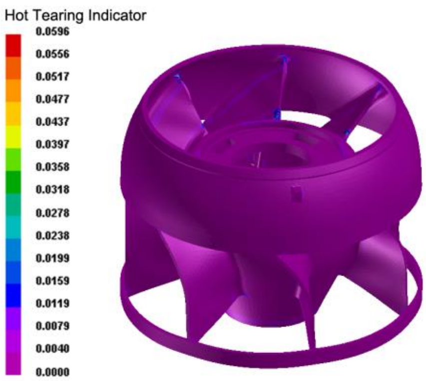

Figure 12. Hot tearing indicator after optimization.

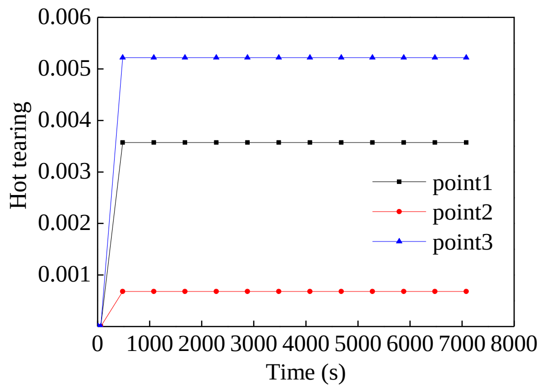

Figure 13. Hot tearing indicator curves after optimization.

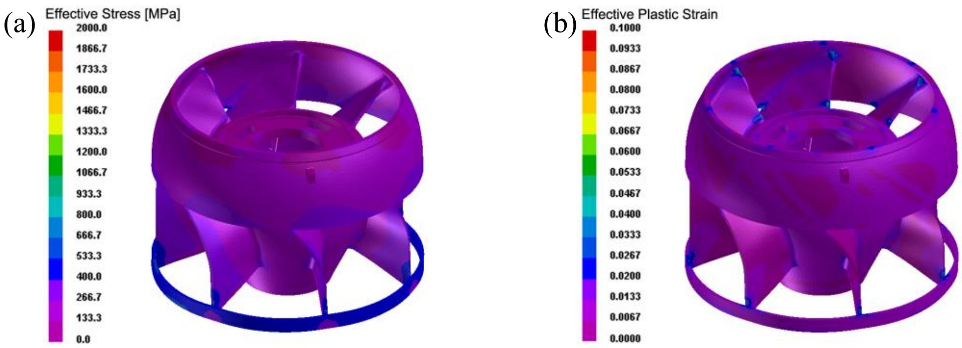

Figure 14. Effective stress and effective plastic strain after optimization. (a) Effective stress, (b) Effective plastic strain.

The effective stress and effective plastic strain after optimization are shown in figure 14. The effective stress and effective plastic strain of T-shape parts are obviously reduced by chills. The Von Mises stress curves after optimization are shown in figure 15. The Von Mises stress of point 1, point 2 and point 3 decrease to 400MPa, 200MPa and 100MPa at 7000s. The effective plastic strain curves after optimization is shown in figure 16. The Von Mises stress of point 1, point 2 and point 3 decrease to 0.020, 0.010 and 0.0006 at time 7000s.

The shrinkage porosity predicted is shown in figure 17. The solidification sequence of T-shaped part is uniform, when the chills are attached on the outer surface of transition regions. The shrinkage porosity is less than without chills.

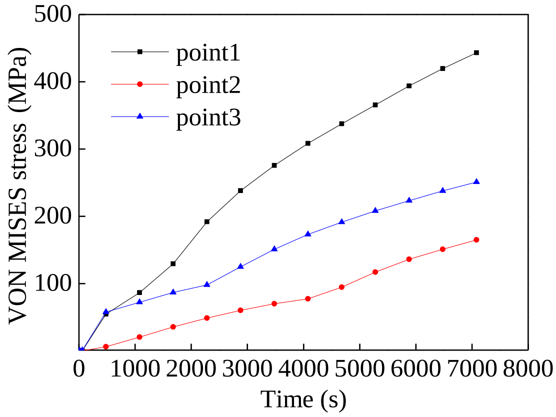

Figure 15. The Von Mises stress curves after optimization.

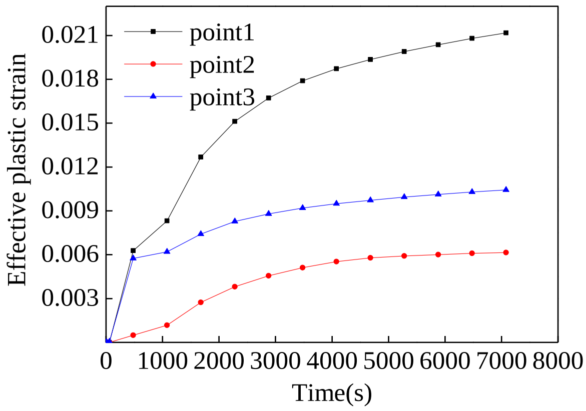

Figure 16. Effective plastic strain curves after optimization.

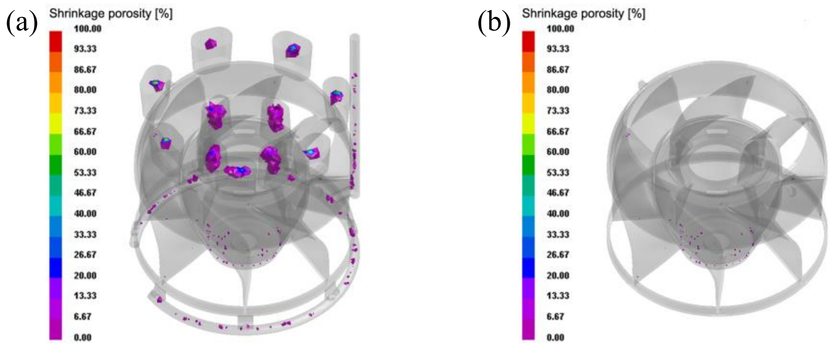

Figure 17. Shrinkage porosity predicted after optimization. (a) Overall view, (b) Partial view.

5. Conclusions

The simulation results of original casting process show that hot tearing tendency is serious at the intersection of blades and outer or inner rings. The shrinkage porosity appears at the bottom of discharge bowl and the transition area of wall thickness. The optimized size parameters of chills range from 25mm to 35mm, and the positions of chills correspond to the outer surface of the T-shaped parts. The hot tearing and shrinkage porosity of the discharge bowl are greatly improved with addition of chills compared with the original casting design (without chills).

Acknowledgments

The authors gratefully acknowledge the financial support from the National Natural Science Foundation of China (Grant No. 51174068 and 51374086).

References

[1] Elin M W, Bengt B and Staffan H 2008 Weldability aspects of a newly developed duplex stainless steel LDX2101 *Mater. Technol* **79** 473-481

[2] Milkowska-Piszczek K and Falkus J 2014 Calculation of the boundary conditions in the continuous casting of steel process *Metalurgija* **53** 571-873
[3] Abdullin A D 2013 Detecting microporosity defects in steel castings by computer modeling of the casting operation in ProCAST *Metallurgis* **57** 167-171
[4] Monroe C, Beckermann C 2005 Development of a hot tear indicator for steel castings *Mat sci eng A-struct* **413** 30-36
[5] Wu M, Sahm P R 1999 Numerical study of porosity in titanium dental castings *J mater sci mater m* **10** 519-525